

Provided for non-commercial research and education use.
Not for reproduction, distribution or commercial use.



This article was published in an Elsevier journal. The attached copy is furnished to the author for non-commercial research and education use, including for instruction at the author's institution, sharing with colleagues and providing to institution administration.

Other uses, including reproduction and distribution, or selling or licensing copies, or posting to personal, institutional or third party websites are prohibited.

In most cases authors are permitted to post their version of the article (e.g. in Word or Tex form) to their personal website or institutional repository. Authors requiring further information regarding Elsevier's archiving and manuscript policies are encouraged to visit:

<http://www.elsevier.com/copyright>



The local threshold for geographical spread of infectious diseases between farms

Gert Jan Boender^{a,*}, Ronald Meester^c, Edo Gies^b,
Mart C.M. De Jong^a

^a *Quantitative Veterinary Epidemiology, Institute of Animal Science and Health (ID-Lelystad),
P.O. Box 65, 8200 AD Lelystad, The Netherlands*

^b *Department of Landscape and Spatial Planning, Alterra Green World Research, Wageningen University
and Research Centre, P.O. Box 47, 6700 AA Wageningen, The Netherlands*

^c *Department of Mathematics, Vrije Universiteit, De Boelelaan 1081A, 1081 HV Amsterdam, The Netherlands*

Received 7 February 2006; received in revised form 9 May 2007; accepted 15 May 2007

Abstract

We investigated the influence of the spatial pattern of farms on the geographical spread of infectious livestock diseases, such as classical swine fever, foot-and-mouth disease and avian influenza in a combined analytical–numerical approach. Our purpose of this paper is to develop a method to identify the areas in which an infection has the potential to spread in an outbreak. In our model, each infected farm can infect neighbouring farms and the probability of transmission is a function of the inter-farm distance (spatial kernel). Therefore, the density of farms in an area is a good indicator for the probability of a major outbreak. In the epidemiological nomenclature, such density corresponds to a local reproduction ratio and we studied the critical behaviour of both the local density and the local reproduction ratio. We found that a threshold can be defined above which major outbreaks can occur, and the threshold value depends on the spatial kernel. Our expression for the threshold value is derived based on scaling arguments and contains two parameters in the exponents of the equation. We estimated these parameters from numerical results for the spatial spread using one particular mathematical function for the form of the spatial kernel. Subsequently, we show that our expression for the threshold using these estimated parameters agrees very well with numerical results for a number of different other functional forms of the spatial kernel (thus suggesting that we are dealing with universal parameters). As an illustration of the practical relevance of the presented method, we calculated the threshold value for avian influenza in the Netherlands and use it to produce a risk map for this disease. © 2007 Elsevier B.V. All rights reserved.

Keywords: Veterinary epidemiology; Spatial spread; Spatial kernel; High-risk areas

* Corresponding author. Tel.: +31 320 238543; fax: +31 320 238961.

E-mail address: gertjan.boender@wur.nl (G.J. Boender).

1. Introduction

Infectious diseases of farmed animals that can be transmitted between farms in the absence of animal movements between those farms are difficult and expensive to combat. Examples are foot-and-mouth disease (FMD), classical swine fever (CSF) and avian influenza (AI) (Ferguson et al., 2001; Stegeman et al., 2002; Ehlers et al., 2003). Control measures for these infections are aimed at stopping between-farm transmission by culling or vaccination of whole farms in areas surrounding infected farms.

Quantitative insight in the effect on transmission is necessary, to guide the design of such control measures. For this purpose simple mathematical models are used that attempt to reflect only the essence of the transmission problem. For example, the vaccination coverage required to eradicate measles in humans was first calculated using a simple model (Anderson and May, 1982). The model they used was based on the assumption of homogeneous mixing (i.e., neglecting preferential contacts) among a large number of individuals. Because of this large number a deterministic description (neglecting stochastic effects) was sufficient.

In the case of farm-to-farm transmission, the spatial structure is important. The assumption of homogeneous mixing is not valid and the preferential-contact structure with a small number of neighbours should be incorporated into the model. And, because of this small number, stochastic effects should be taken into account. Therefore, we introduced a spatial and stochastic transmission model defined as follows. If r_{ij} denotes the distance between farm i and farm j , the probability that farm i (if infected) will transmit the infection to farm j is given by a spatial kernel $p(r_{ij})$. This spatial kernel $p(r_{ij})$ summarises the probability of transmission without specifying the routes of infection, and is only a function of the Euclidean distance (i.e., straight-line distance) between the farms. Strong support for the choice of Euclidean distance as opposed to alternative, more complicated, distance measures (e.g., shortest or quickest routes between the farms) is provided by an analysis by Savill et al. (2006). Analysing the large and detailed data arising from the 2001 FMD epidemic in Great Britain, they concluded that a simple spatial kernel based on Euclidean distance sufficed in most regions to predict the transmission between infectious and susceptible farms. Our model can be described as a special kind of percolation problem, thus allowing us to borrow insights from percolation theory (Meester and Roy, 1996; Stauffer and Aharony, 1994). This mathematical theory deals with random connected networks. The basic result of percolation theory is the existence of a sharp phase transition at which the long-range connectivity of the network appears. This transition occurs abruptly when some generalized density in this system reaches a critical value (critical point). To arrive at a percolation-problem formulation, we viewed the set of farms as a network of nodes, while the spatial kernel $p(r_{ij})$ was interpreted as the probability that node i and j become connected. The important question was: for which conditions does percolation occur upon invasion? In the terminology of epidemiology, this question read: in which areas can an introduction of an infection lead to a major outbreak?

As yet, there was no analytical framework available to answer this question by calculation of the critical point for such a system. Therefore, we first had to develop a methodology to estimate critical points for spatial spread of infections. We reached this goal in three steps, as described in the theoretical part below:

- (1) We suggested an approximate mathematical expression of the critical point, based on scaling arguments.

Table 1
Notation

Symbol	Description	Unit
ε	Deviance from the averaged probability of transmission, Eq. (8)	Unitless
i	Farm index	Unitless
j	Farm index	Unitless
λ	Density of farms	km ⁻²
λ_c	Critical density of farms	km ⁻²
λ_{hi}	Local density around farm i	km ⁻²
p_0	Maximum probability of transmission, Eqs. (6)–(9)	Unitless
p	Spatial kernel	Unitless
\bar{p}	Intensity (the zeroth moment) of the spatial kernel p , Eq. (3)	km
$\langle r \rangle$	Spatial dispersion (the first moment) of the spatial kernel p , Eq. (3)	km
$\langle \frac{1}{2}r^2 \rangle$	Second moment of the spatial kernel p	km ²
r	Distance	km
r'	Integration variable, Eq. (3)	km
r_{ij}	Distance between farm i and farm j	km
r_s	Scaling distance, Eqs. (6)–(9)	km
R	Reproduction ratio	Unitless
R_0	Reproduction ratio in a susceptible population	Unitless
R_c	Critical value of the reproduction ratio	Unitless
R_h	Reproduction ratio in the case of spatial spread between farms (in case of a homogeneous farm density)	Unitless
R_{hi}	Reproduction ratio of farm i in the case of spatial spread between farms (non-homogeneous farm density)	Unitless
q	Exponential power, Eq. (6)	Unitless
x	Replacement factor, Eq. (9)	Unitless
y	Coefficient, Eq. (5)	Unitless
z	Coefficient, Eq. (5)	Unitless

- (2) We estimated the parameters in this expression via numerical calculation of an outbreak in a set of complete spatially random-distributed farms in a plane (a two-dimensional Poisson point process), leading to a critical point for a given spatial kernel.
- (3) We validated this expression via comparison of the predicted value for the critical point according to this expression to the numerical results we obtained using other spatial kernels.

As an illustrative application of this methodology, we used a spatial kernel estimated for AI and the heterogeneous distribution of poultry flocks in the Netherlands to determine the high-risk areas for AI in the Netherlands and compared the results with data of the AI outbreak in the Netherlands in 2003.

For reference we provide a list of notation in Table 1.

2. Methods

First, using the terminology of percolation theory, we described the spread of an infectious disease between farms in a network of nodes in which the probability that a connection between node i and j takes place equals the spatial kernel $p(r_{ij})$, where r_{ij} denotes the distance between i and j . We assumed that the transmission is homogeneous (implying that p is a not function of the position of the farm, but only a function of the relative distance), and is isotropic (i.e., directionally independent). With these assumptions p is only a function of the distance r_{ij}

between the two points i and j . We also assumed that the farm can be represented by a single point, neglecting the spatial extent of the premises.

Because an analytical solution for the critical point as a function of the spatial kernel is not available, we chose a numerical approach to simulate the critical point using the software package Mathematica (Wolfram, 1999). In our approach, we started with set of nodes in the two-dimensional plane. Thereafter we declared one single farm infected (to represent the first infectious farm in the epidemic). In the random process of transmission the infection from the first infected farm i to farm j governed by the spatial kernel $p(r_{ij})$, other nodes became connected to this first infected node, and these nodes formed the next generation of infections. After this, we repeated the procedure for the new set of nodes, leading to a network of connected nodes (representing the set of infected farms). Note that we simulated the spread of the infectious disease not in real time but in generations of infected farms. The final size of the epidemic corresponds to the total number of connected nodes.

As mentioned above, the spatial kernel $p(r_{ij})$ is the probability that an infected farm i infects another farm j at a distance r_{ij} during its period of infectiousness. It is possible to estimate these spatial kernels from data of epidemics (Stegeman et al., 1999, 2002; Ferguson et al., 2001). We stress that such a function is always measured in the presence of a certain set of intervention measures; the set often included the prohibition of between-farm movement of animals. A change in intervention measures might lead to a different spatial function.

In this theoretical part, we focussed on a set of nodes generated by a Poisson point process for a given density λ . This gave us the opportunity to study the effect of the density on the spatial spread of the infection. In epidemiology the concept of the reproduction ratio R is used to quantify the transmission intensity, where R_0 is defined as the averaged number of infected farms by one typical infectious farm in a completely susceptible population (Diekmann et al., 1990). Using this definition, we constructed a reproduction ratio R_h pertaining to spatial spread between farms. For a set of complete spatially random-distributed nodes in a plane with density λ , the expected number of nodes in a ring of (infinitesimally small) thickness dr and with radius r around an arbitrarily chosen node, is $\lambda 2\pi r dr$. For an infectious node in the centre of the ring, each node in this ring had the probability $p(r)$ to become infected. The expected number of infected nodes in this ring thus is equal to $\lambda \pi p(r) \pi r dr$. Because the density λ is independent of r , the total expected number of infected nodes sums up to:

$$R_h = \lambda \int_0^{\infty} p(r) 2\pi r dr \quad (1)$$

In this equation, R_h gives the expected number of infected farms in each generation, as long as the number of infected farms in the neighbourhood of the infectious farm remains negligible with respect to the number of susceptible farms. Strictly speaking, this is not true, because for each infected farm there is at least one neighbour already infected, i.e., the one that had infected the infected farm we were considering. Ignoring this, then a threshold ($R_h = 1$) exists. Above this threshold ($R_h > 1$) the infection can invade, while in the complimentary case ($R_h < 1$) the infection cannot. However, in the case of local spread, the number of infected farms in the neighbourhood of an one infectious farm is in general not negligible, and local depletion of the susceptible pool could lead to a self-limiting outbreak, even when $R_h > 1$ (Levin and Durrett, 1996). The central question we address in this paper is at which threshold for R_h the infection would continue to spread, if local depletion is not ignored.

We used the relationship between λ and R_h in Eq. (1) to represent this dependence on local depletion of susceptibles. Also in the presence of local depletion, (local) density is important, because percolation theory predicts the existence of a critical density λ_c indicating a phase transition from small-connected networks (minor outbreaks) to a large connected network (major outbreak) (see, e.g., Meester and Roy, 1996). According to the relationship between λ and R_h in Eq. (1) the existence of λ_c corresponds to the existence of critical reproduction ratio R_c . For $R_h > R_c$, major outbreaks can occur, while for $R_h < R_c$ only minor outbreaks can occur.

Although λ and R_h appeared to be interchangeable variables according to Eq. (1), we preferred to use R_h as the basic variable. There are several arguments to do so:

- (1) This paper presents an epidemiological description and we wanted to use the nomenclature of this field. In epidemiology R is used, because this variable not only reflects the properties of the population, but also the spread of the infection. In the same way the R_h given in Eq. (1) both reflects the spatial density and the spatial kernel essential to the description of spatial spread.
- (2) R_h is independent of the chosen unit of distance (km, miles), leading to an unambiguous interpretation of numbers.
- (3) In the next section, we want to use this concept in the situation without a homogeneous density. In that case it is still straightforward to define a *local reproduction ratio*.

Each farm j at distance r_{ij} has the probability $p(r_{ij})$ to become infected by an infectious farm i . The total averaged number of infected farms sums up to the local reproduction ratio of farm i :

$$R_{hi} = \sum_{j \neq i} p(r_{ij}) \tag{2}$$

Using this definition of R_{hi} and the relationship between density and reproduction ratio in Eq. (1), it will be possible to derive a local density λ_{hi} . This local density is fully determined by the spatial kernel (describing the transmission of the infection) without the need to choose an arbitrary bandwidth as usual in GIS analyses (Bailey and Gatrell, 1996).

In the following we discuss a methodology to estimate R_c ; this value should be larger than 1, although the exact value will depend on the spatial kernel $p(r)$.

- (1) The first step is to find an approximate closed-form expression for R_c in terms of $p(r)$. To characterize of the spatial kernel, we used the moments of $p(r)$:

Moment	Formula	Spatial dimension	
0	$\bar{p} = \int_0^\infty p(r') dr'$	1	
1	$\langle r \rangle = \int_0^\infty \frac{p(r')}{\bar{p}} r' dr'$	1	(3)
2	$\langle \frac{1}{2}r^2 \rangle = \int_0^\infty \frac{p(r')}{\bar{p}} \frac{1}{2}r'^2 dr'$	2	

in which \bar{p} is the intensity, $\langle r \rangle$ the spatial dispersion and $\langle \frac{1}{2}r^2 \rangle$ the second moment of $p(r)$, such that $\bar{p}\langle r \rangle$ is a measure of the total infectivity. To construct an approximate expression for R_c from these moments, we used dimension analysis and scaling properties (Zlokarnik, 1991). Because the reproduction ratio should be independent of the chosen unit of distance, it must be written as a function of dimensionless parameters. The simplest dimensionless

parameters were:

$$\frac{\bar{p}}{\langle r \rangle} \text{ and } \frac{\langle r \rangle^2}{\langle \frac{1}{2}r^2 \rangle} \quad (4)$$

We sought to express R_c as a function of these two quantities, assuming that they are sufficient to describe the behaviour of the R_c and that higher-order factors can be neglected. Anticipating certain scaling properties for the deviation from 1 of the critical reproduction ratio, R_c is written as a scaling function:

$$R_c = 1 + \left(\frac{\langle r \rangle^2}{\langle \frac{1}{2}r^2 \rangle} \right)^z \left(\frac{\bar{p}}{\langle r \rangle} \right)^y \quad (5)$$

where z and y are constant. We estimated the values of z and y by numerical calculations of critical points using the software package Mathematica (Wolfram, 1999) as discussed above.

(2) The second step is the numerical estimation of the coefficients y and z for a specific spatial kernel. The spatial kernel we used was:

$$p(r) = p_0 \exp\left(-\left(\frac{r}{r_s}\right)^q\right) \quad (6)$$

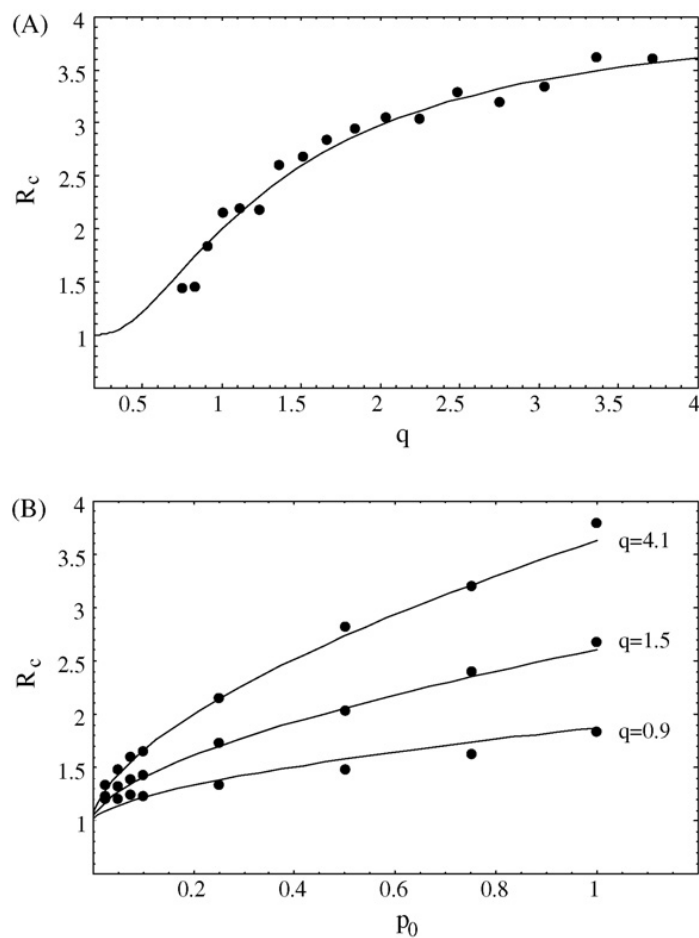


Fig. 1. (A) The critical reproduction ratio R_c for the spatial kernel given in Eq. (6) as function of the power exponent q ($p_0 = 1$). (B) The critical reproduction ratio R_c for the same spatial kernel as function of the maximal probability of transmission p_0 ($q = 4.1, 1.5, 0.9$). The dots are simulated points, while the solid line is the theoretical curve.

in which r_s is the scaling distance, q the exponential power, while p_0 is the probability of transmission at $r = 0$. It is possible to vary this function from a fully local limit ($q \rightarrow \infty$) to a non-spatial limit ($q \rightarrow 0$) (Ferguson et al., 2001). In the second limit $R_c \rightarrow 1$, as expected for random mixing. Using this kernel, we estimated λ_c of a Poisson point process through numerical calculations for different values of q and p_0 . Subsequently, we calculated R_c from λ_c according to Eq. (1). Finally, we obtained the estimates $z \approx 1.7$ and $y \approx 0.6$ via comparison of these values with the expression for R_c given in Eq. (5). In Fig. 1A, R_c as a function of q is shown for the extreme $p_0 = 1$, while the solid line is calculated using Eqs. (5) and (6). In Fig. 1B, R_c as a function of p_0 is shown for several values of q .

- (3) The third step is validation of the universality of this expression (with the estimates $z \approx 1.7$ and $y \approx 0.6$) via numerical calculations using other spatial kernels.
- (a) First, we considered the spatial kernel:

$$p(r) = \begin{cases} p_0 \left(1 - \left(\frac{r}{r_s} \right)^2 \right)^2 & r \leq r_s \\ 0 & r > r_s \end{cases} \quad (7)$$

in which r_s is the scaling distance, while p_0 is the probability of transmission at $r = 0$. Such a spatial kernel is often used often in GIS analysis (Bailey and Gatrell, 1996). In Fig. 2, R_c as a function of p_0 is shown, while the solid line corresponds to the expression given in Eq. (5) using the spatial kernel given in Eq. (7), without further adjustment.

- (b) Secondly, we considered a spatial kernel of a type that has been used in the analysis of epidemiological data (e.g., Stegeman et al., 2002). Such a spatial kernel assigns transmission probabilities to a discrete set of distance ranges:

$$p(r) = \begin{cases} p_0 \left(\frac{1}{2} + \varepsilon \frac{1}{2} \right) & r \leq \frac{1}{3} r_s \\ p_0 \frac{1}{2} & \frac{1}{3} r_s < r \leq \frac{2}{3} r_s \\ p_0 \left(\frac{1}{2} - \varepsilon \frac{1}{10} \right) & \frac{2}{3} r_s < r \leq r_s \\ 0 & r_s < r \end{cases} \quad (8)$$

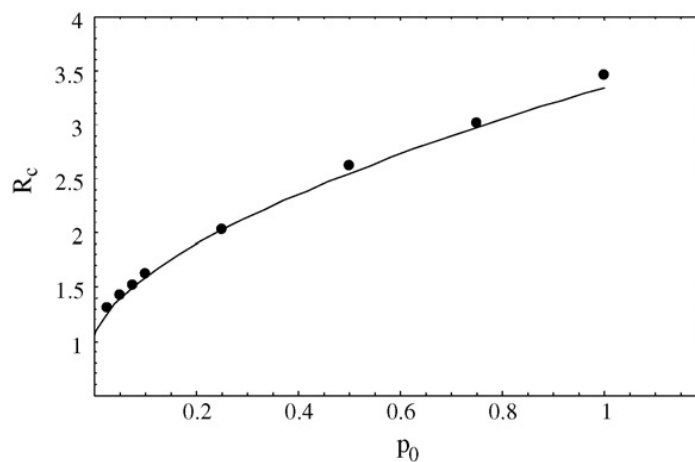


Fig. 2. The critical reproduction ratio R_c for the spatial kernel given in Eq. (7) as the maximal probability of transmission p_0 . The dots are simulated points, while the solid line is the theoretical curve.

in which r_s is the scaling distance, p_0 is the probability of transmission at $r = 0$ and $\varepsilon = 1$, and ε is a parameter describing the deviance from the average probability of transmission $\frac{1}{2}p_0$ in the different distance ranges ($0 \leq \varepsilon \leq 1$). Substitution of Eq. (8) into Eq. (1) gives $R_c = \frac{1}{2}p_0\pi r_s^2\lambda_c$, independent of the parameter ε . In Fig. 3A, R_c as a function of ε is shown for the extreme $p_0 = 1$ and in Fig. 3B, R_c as a function of p_0 is shown for the maximum deviance $\varepsilon = 1$. The solid line is calculated using the Eqs. (5) and (8).

(c) Thirdly, we considered a spatial kernel that does not have its highest probability around the origin. We included this case to check whether it is essential for the validity of the expression given in Eq. (5) that $p(r)$ is monotonically decreasing with distance. The spatial kernel is:

$$p(r) = p_0 \exp\left(-\left(\frac{r}{r_s} - x\right)^2\right) \quad (9)$$

in which r_s is the scaling distance, p_0 is the probability of transmission at $r = 0$ and $x = 0$ and x is the replacement factor (in units of r_s). The replacement factor x describes how much the maximum of the spatial kernel is shifted away from the centre ($r = 0$). In Fig. 4A, R_c as a function of x is shown for the extreme $p_0 = 1$ and in Fig. 4B, R_c as a function of p_0 is shown for $x = 1$ (the replacement equalled r_s). The solid line is calculated using the Eqs. (5) and (9).

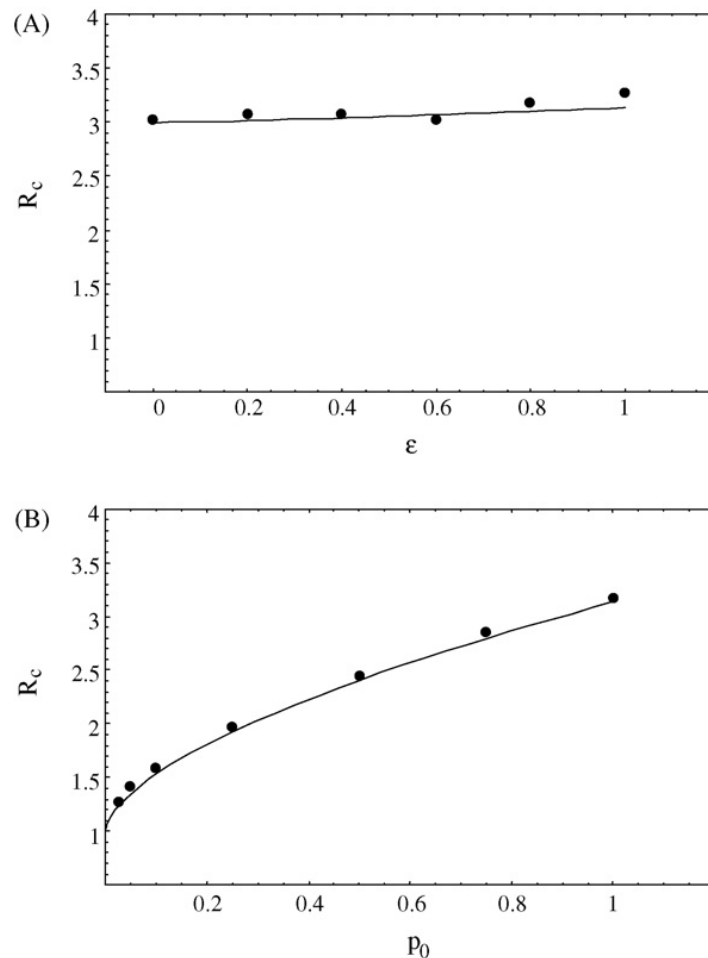


Fig. 3. (A) The critical reproduction ratio R_c for the spatial kernel given in Eq. (8) as function of the deviation factor ε ($p_0 = 1$). (B) The critical reproduction ratio R_c for the same spatial kernel as the maximal probability of transmission p_0 ($\varepsilon = 1$). The dots are simulated points, while the solid line is the theoretical curve.

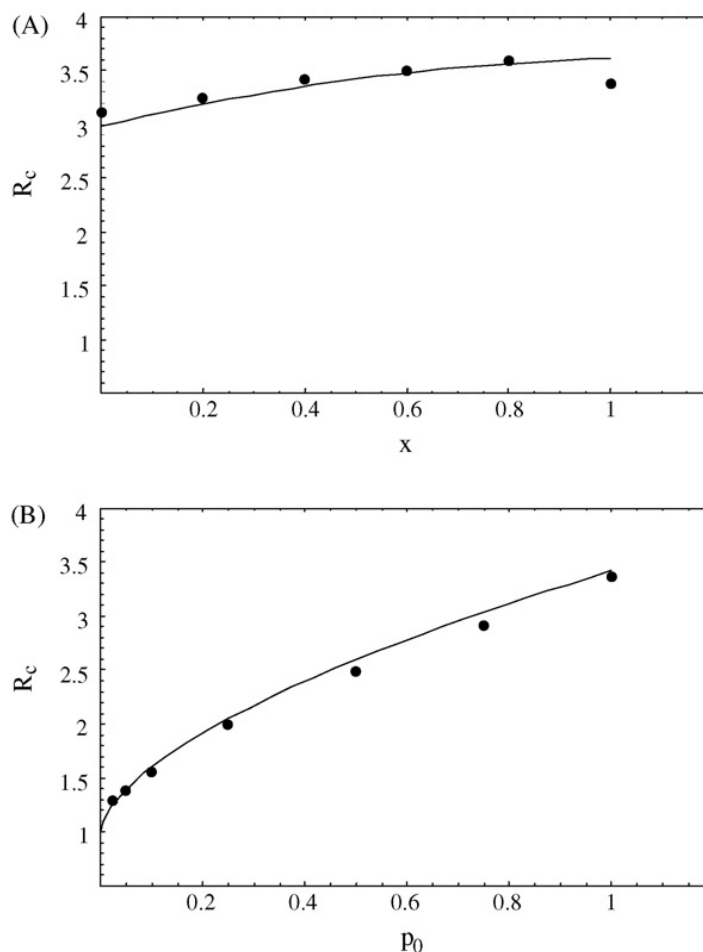


Fig. 4. (A) The critical reproduction ratio R_c for the spatial kernel given in Eq. (9) as function of the replacement factor x ($p_0 = 1$). (B) The critical reproduction ratio R_c for the same spatial kernel as the maximal probability of transmission p_0 ($x = 1$). The dots are simulated points, while the solid line is the theoretical curve.

Based on this extensive validation, using this variety of spatial kernels, we have obtained sufficient confidence in the universality of the expression given in Eq. (5).

3. Results

To illustrate how this method could be applied we considered the epidemic of AI in the Netherlands in 2003 (Stegeman et al., 2004). At the start of this epidemic no detailed information about the spatial spread of AI in the Netherlands was available. Following the approach used for analysing an AI epidemic in Italy (Ehlers et al., 2003), we assumed a spatial kernel of the form given in Eq. (7). We used the data of the first cases of the AI outbreak in the Netherlands. We assumed that each infected flock was infected by the nearest infectious flock. It appeared that most of the transmission of the infection took place within about 5 km and about 1 out of 20 neighbouring flocks became infected by an infectious flock. In this way we arrived at an estimate of 5 km for r_s and an estimate of 0.05 for p_0 . Subsequently we used this spatial kernel and the set of locations of poultry flocks in the Netherlands to calculate the local reproduction ratio R_{hi} and identify high-risk areas as those areas where R_{hi} exceed the critical value R_c obtained from the presented methodology. We could have calculated R_{hi} for each flock i to identify high-risk areas. In this case we would use the flock locations as sampling points for the local reproduction ratio.

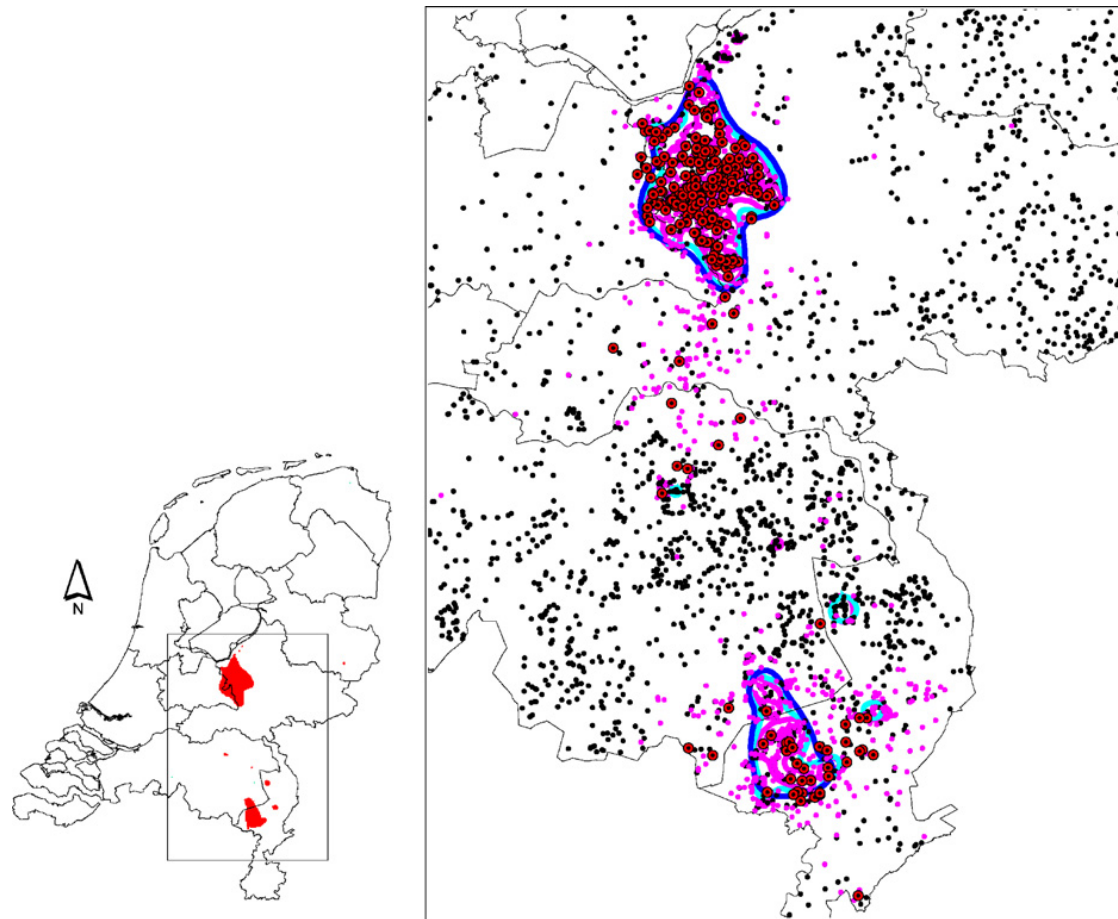


Fig. 5. Map with an estimate of the high-risk areas (red) for spatial spread of Avian Influenza in the Netherlands. An enlargement of the relevant part containing high-risk areas for a maximum probability of transmission p_0 of 0.14 and a scaling radius r_s of 3 km (pink), for p_0 of 0.05 and r_s of 5 km (light blue) and for p_0 of 0.026 and r_s of 7 km (dark blue). The red dots in the enlargement are cases of the 2003 AI-epidemic, the black dots the uninfected flocks, while the pink dots are the preventively removed flocks. (For interpretation of the references to colour in this figure legend, the reader is referred to the web version of the article.)

However, we used a readily available GIS-routine, which used grid points as sampling points (Press et al., 1986). The high-risk area for AI in the Netherlands is shown in Fig. 5. On one hand, we observed in this map produced by our method two main high-risk areas. On the other hand, we observed at the same time in the actual outbreak the infection was spreading only in the northern high-risk area, while outside this high-risk area the infection did not propagate locally. However, a few days later in the actual outbreak the infection was introduced in the southern high-risk area, where it was spreading too. The correspondence of both observations gave us great confidence in the validity of the risk-map calculation. It can be shown how to use robust estimation methods to obtain the spatial kernel. We discuss this issue in a separate publication, together with further evidence for the predictive validity of the risk-map approach (Boender et al., 2007).

We have carried out some additional calculations to obtain an idea of the sensitivity of the size of the high-risk areas with respect to the parameters r_s ($= 5$ km) and p_0 ($= 0.05$). In Fig. 5, we show the high-risk areas for $r_s = 3, 5, \text{ and } 7$ km, keeping the reproduction ratio constant according to Eq. (1). We compared these high-risk areas to the actual infected flocks in the 2003 AI epidemic in the Netherlands. In the high-areas (for $r_s = 5$ km) 191 of the 1440 flocks were infected, while 237 flocks were infected in the total Dutch poultry population of 5705 flocks. The much higher proportion of infected flocks in the high-areas, confirmed with rejecting equal

proportion via a Fischer Exact Test ($p < 0.001$), is fully consistent with our assignment of high-risk areas. As a consequence of varying the scaling distance with 80% (from $r_s = 3$ km to $r_s = 7$ km) the number of flocks in the high-risk areas varied only with 6% (from 1385 to 1468).

4. Discussion

We observed that in Fig. 1, the expression for R_c given in Eq. (5) was a good approximation for $z \approx 1.7$ and $y \approx 0.6$, because the theoretical curve for R_c agreed with the simulated values for R_c .

The validation of the expression for R_c in the previous section shows that the use of R_c is not restricted to calculations of critical densities with the spatial kernel in Eq. (6) (which we used to estimate the parameters $y \approx 0.6$ and $z \approx 1.7$), but is valid for calculations of critical densities with other spatial kernels as well.

The application of the methodology to construct a risk map for AI in the Netherlands is illustrated in Fig. 5. We also note that the three sets of high-risk areas calculated using three different sets of parameters for the spatial kernel overlap to a great extent. We show that the size of the high-risk areas is not very sensitive to uncertainties in the parameters of the spatial kernel. This last conclusion might be partly due to sharp clustering of poultry farm locations in the Netherlands. The presented results give confidence in the usefulness of the risk map as a concise and understandable approach in spatial epidemic planning. An example is the planning of spatially dependent measures to control an outbreak. The spatial kernel used can be obtained from the analyses of a previous epidemic. We obtained a good identification of high-risk areas even with a spatial kernel estimated from the available data of the current epidemic. In a high-risk area the epidemic will not self-extinguish and additional interventions are necessary to halt the epidemic spread. However, which epidemic size is acceptable and which measures should be taken is not only a matter of epidemiology, because economical and political factors also are involved.

Our approach gives several directions for further research:

- (1) The border of a high-risk area is probably not sharp but could have certain width. Further investigations are needed to elucidate the risk profile of the border.
- (2) The expression in Eq. (5) is based on scaling arguments and not on an analytical theory. Such a mathematical theory might provide a derivation of the coefficients y and z from underlying properties of the system, and also indicate for which spatial kernels this expression is a reasonable approximation.
- (3) Our methodology enables the identification of high-risk areas for epidemic spread, in which additional intervention measures are required to halt epidemic spread. It does not describe how much additional effort would be required. Time-dependent modelling of the spread in high-risk areas under different intervention strategies can be used to obtain insight into this question and to inform the design of control strategies.

5. Conclusions

We can conclude that the estimate of R_c given in Eq. (5) predicts the critical point for the possible incidence of major outbreaks for a variety of spatial kernels given in Eqs. (7)–(9). This methodology has enabled us to construct risk maps for the geographical spread of infectious diseases between farms. The correspondence of the high-risk areas on the map of the Netherlands with the actual AI epidemic was remarkably good.

Acknowledgement

We thank Thomas Hagenaars for useful comments on the manuscript.

References

- Anderson, R.M., May, R.M., 1982. Directly transmitted infectious diseases: control by vaccination. *Science* 215, 1053–1060.
- Bailey, T.C., Gatrell, A.C., 1996. *Interactive Spatial Data Analysis*. Longman, Harlow.
- Boender, G.J., Hagenaars, T.J., Bouma, A., Nodelijk, G., Elbers, A.R.W., de Jong, M.C.M., van Boven, M., 2007. Risk maps for the spread of highly pathogenic avian influenza in poultry. *PLoS Comput. Biol.* 3 (4): e71, doi:10.1371/journal.pcbi.0030071.
- Diekmann, O., Heesterbeek, J.A.P., Metz, J.A.J., 1990. On the definition and the computation of the basic reproduction ratio R_0 in models for infectious diseases in heterogeneous populations. *J. Math. Biol.* 28, 365–382.
- Ehlers, M., Möller, M., Marangon, S., Ferre, N., 2003. The use of Geographic Information System (GIS) in the Frame of the Contingency Plan Implemented During the 1999–2001 Avian Influenza (AI) Epidemic in Italy. *Avian Dis.* 47, 1010–1014.
- Ferguson, N.M., Donnelly, C.A., Anderson, R.M., 2001. The Foot-and-Mouth Epidemic in Great Britain: pattern of spread and impact of interventions. *Science* 292, 1155–1160.
- Levin, S.A., Durrett, R., 1996. From individuals to epidemics. *Philos. Trans. R. Soc. Lond. B* 351, 1615–1621.
- Meester, R., Roy, R., 1996. *Continuum Percolation*. Cambridge University Press, Cambridge.
- Press, W.H., Flannery, B.P., Teukolsky, S.A., Vetterling, W.T., 1986. *Numerical Recipes: The art of scientific Computing*. Cambridge University Press, New York.
- Savill, J.N., Shaw, D.J., Deardon, R., Tildesley, M.J., Keeling, M.J., Woolhouse, M.E.J., et al., 2006. Topographic determinants of foot and mouth disease transmission in the UK 2001 epidemic. *BMC Vet. Res.* 2, 3.
- Stauffer, D., Aharony, A., 1994. *Introduction to Percolation Theory*. Taylor & Francis, London.
- Stegeman, J.A., Elbers, A.R.W., Smak, J., de Jong, M.C.M., 1999. Quantification of the transmission of classical swine fever virus between herds during the 1997–1998 epidemic in the Netherlands. *Prev. Vet. Med.* 42, 219–234.
- Stegeman, J.A., Elbers, A.R.W., Bouma, A., de Jong, M.C.M., 2002. Rate of inter-herd transmission of classical swine fever virus by different types of contact during the 1997–1998 epidemic in the Netherlands. *Epidemiol. Infect.* 128, 285–291.
- Stegeman, J.A., Elbers, A.R.W., Bouma, A., de Jong, M.C.M., Nodelijk, G., de Klerk, F., et al., 2004. Avian influenza A virus (H7N7) epidemic in the Netherlands in 2003: course of the epidemic and effectiveness of control measures. *J. Infect. Dis.* 190, 2088–2095.
- Wolfram, S., 1999. *Mathematica*, 4th ed. Wolfram Media.
- Zlokarnik, M., 1991. *Dimensional Analysis and Scale-up in Chemical Engineering*. Springer-Verlag, Berlin.